

Article

Not peer-reviewed version

The Transverse Momentum Distribution of J/ψ Mesons Produced in Pp Collisions at the LHC

[Lina Gao](#)^{*} and [Erqin Wang](#)

Posted Date: 14 March 2023

doi: 10.20944/preprints202303.0240.v1

Keywords: the modified Hagedorn function; J/ψ mesons; transverse momentum distribution



Preprints.org is a free multidiscipline platform providing preprint service that is dedicated to making early versions of research outputs permanently available and citable. Preprints posted at Preprints.org appear in Web of Science, Crossref, Google Scholar, Scilit, Europe PMC.

Copyright: This is an open access article distributed under the Creative Commons Attribution License which permits unrestricted use, distribution, and reproduction in any medium, provided the original work is properly cited.

Article

The Transverse Momentum Distribution of J/ψ Mesons Produced in pp Collisions at the LHC

Li-Na Gao * and Er-Qin Wang

Department of Physics, Taiyuan Normal University, Jinzhong, Shanxi 030619, China

* Correspondence: 114433833@qq.com

Abstract: The transverse momentum distribution of J/ψ mesons produced in pp collisions at the center-of-mass energy 5 TeV, 7 TeV, and 13 TeV is described by the modified Hagedorn function which is based on the Tsallis function and Hagedorn function. The calculated results by the modified Hagedorn function are in accord with experimental data measured by the LHCb Collaboration at LHC. The related parameters are obtained and analyzed.

Keywords: the modified Hagedorn function; J/ψ mesons; transverse momentum distribution

1. Introduction

More and more scientific workers get involved in exploring the origin of the universe. According to modern cosmology, the quark-gluon plasma (QGP) is the initial state after the Big Bang and the original state of matter. So, exploring and studying the QGP is a way to understand the universe's evolution. In the extremely high temperature and high-density particle collision area may be production the QGP. In the experimental, accelerated the speed of the two antithetical heavy nuclei approach the speed of light and have a central collision to be formed a small 'big bang' and produced the QGP. Creating and studying the QGP has become the main goal of the high energy heavy ion collision experiment. But, the new form of nuclear matter (QGP) cannot be directly observed by the detectors. We can only analyze the final particles of relativistic heavy ion collisions to infer the properties of QGP. To date, we have got a lot of experimental data provided by the Relativistic Heavy Ion Collider (RHIC) and the Large Hadron Collider (LHC) to study. And, scientists have obtained some achievements about the QCD diagram and nuclear matter [1,2].

In the whole process of collision, the collision system is emitted particles and nuclear fragments constantly. The kinds and dynamical properties of the particles and nuclear fragments emitted at different stages are not the same. Therefore, the final products of collisions have carried on a lot of the evolution information of collision progress [3]. The transverse momentum distribution of final state particles is an important object of observation in the experimentally, it can provide more important information to study the kinetic freezing temperature, the radial velocity of particles, chemical potential, the transverse excitation degree of collision system, and so on. In this paper, we described the transverse momentum distribution of J/ψ mesons produced in pp collisions at different collision energy, extracted and analyzed some related parameters.

2. The model and method

In our previous work [4–8], we have revised some thermodynamic statistical distributions based on the multisource thermal model. In the work [4,5], we put forward two components of statistical models which are the two-component Elang distribution and the two-component Schwinger mechanism. We used the two revised model to analyze the transverse momentum distributions of ϕ mesons, Ω hyperons, and negatively charged particles produced in Au-Au collisions with different centrality intervals, measured by the STAR Collaboration at 7.7 GeV, 11.5 GeV, 19.6 GeV, 27 GeV, and 39 GeV in the beam energy scan program at RHIC. And, we used the two methods to study the transverse momentum spectra of J/ψ and Υ mesons produced in pp , p -Pb, Pb-Pb collisions measured

by LHCb and ALICE Collaboration at LHC. In the work [6], we structured a two-component statistical model which is a super position of the Tsallis statistics and the inverse power law. We used this two-component statistical model to analyze the transverse momentum distributions of J/ψ and Υ mesons produced in pp , p -Pb collisions at 5 TeV, 7 TeV, 8 TeV, and 13 TeV measured by LHCb Collaboration at LHC. In the work [7], We used two models (the two-component Schwinger mechanism and the two-component statistical model which is based on the Tsallis statistics and the inverse power law) to study the Λ_c^+ , Λ_b^0 baryons, D^0 , \bar{B}^0 mesons and some related particles produced in pp , p -Pb collisions at 5 TeV, 7 TeV, 8 TeV, and 13 TeV. From our prophase related work, one can see that our revised models could describe the experimental data very well. And based on our revised models, we extracted some related important parameters and analyzed their trend with rapidity and collision energy. Through these studies works, we try to get some useful information about the collision mechanism, the evolution of the collision system and the QGP.

In this work, we use the modified Hagedorn function to study the transverse momentum distribution of J/ψ mesons produced in pp collisions at the center-of-mass energy 5 TeV, 7 TeV, and 13 TeV. To complete this paper, we will introduce this function briefly in the following paragraphs.

In the reference [9,10], the Hagedorn function is written as:

$$\frac{d^2 N}{2\pi N_{ev} p_t dp_t dy} = C \left(1 + \frac{m_t}{p_0} \right)^{-n} \quad (1)$$

In this function, C is the fitting constant, $m_t = \sqrt{p_t^2 + m_0^2}$ denotes the transverse mass, p_0 and n are the free parameters. Based on Quantum Chromodynamics, the Hagedorn function can be described the high transverse momentum part of transverse momentum distributions of hadrons very well.

It is well-known that the Tsallis function is a very useful method to study the transverse momentum of final state particles in pp collisions at RHIC and LHC energy range. The simplest form of the Tsallis function is:

$$\frac{d^2 N}{2\pi N_{ev} p_t dp_t dy} = C_q \left(1 + (q-1) \frac{m_t}{T} \right)^{-1/(q-1)} \quad (2)$$

By comparing the Hagedorn function and Tsallis function, one can see that when the parameter n can be expressed as $1/(q-1)$ and p_0 can be expressed as nT (T is effective temperature), the Hagedorn function and the Tsallis function are mathematically equivalent. So, we could revise function (1) to

$$\frac{d^2 N}{2\pi N_{ev} p_t dp_t dy} = C \left(1 + \frac{m_t}{nT_0} \right)^{-n} \quad (3)$$

In the references [11–14], m_t can be transform to $\langle \gamma_t \rangle (m_t - p_t \langle \beta_t \rangle)$, and $\langle \gamma_t \rangle = \frac{1}{\sqrt{1 - \langle \beta_t \rangle^2}}$. In

this way, function (3) can be written as

$$\frac{d^2 N}{2\pi N_{ev} p_t dp_t dy} = C \left(1 + \langle \gamma_t \rangle \frac{(m_t - p_t \langle \beta_t \rangle)}{nT_0} \right)^{-n} \quad (4)$$

Function (4) is the form of the modified Hagedorn function. We have used the function (4) to study the transverse momentum distribution of J/ψ mesons produced in pp collisions at 5 TeV, 7 TeV, 8 TeV, and 13 TeV measured by LHCb Collaboration at LHC. The following section introduced the details of our research work.

3. Results and discussion

Figure 1 shows the transverse momentum distribution of J/ψ mesons produced in pp collisions at $\sqrt{s}=5$ TeV. Figure 1(a) presents the results of prompt J/ψ mesons and Figure 1(b) present the results of nonprompt J/ψ mesons, respectively. The hollow symbols with the error bars represent the experimental data measured by the LHCb Collaboration in literature [15], the different rapidity ranges are denoted by different symbols in the panels. The solid curves are our results calculated by the modified Hagedorn function. The values of free parameters (n , T_0 , β_t) and degree of freedom (χ^2/dof) corresponding to each curve in Figure 1 are listed in Table 1. One can see that the modified Hagedorn function could describe the experimental data measured in pp collisions at the center-of-mass energy 5 TeV by the LHCb Collaboration. The trends of parameters on the rapidity will be discussed later.

Figures 2 and 3 are similar to Figure 1. Figure 2 show the transverse momentum spectra of 2(a) prompt J/ψ , 2(b) J/ψ from b, 2(c) prompt J/ψ with fully transversely polarized, 2(d) prompt J/ψ with fully longitudinally polarized in pp collisions at $\sqrt{s}=7$ TeV, respectively. Figures 3(a) and 3(b) show the results of prompt J/ψ and J/ψ from b mesons in pp collisions at $\sqrt{s}=13$ TeV, respectively. The hollow symbols with the error bars represent the experimental data measured by the LHCb Collaboration in literatures [16,17]. The solid curves are our results calculated by the modified Hagedorn function. The values of free parameters (n , T_0 , β_t) and degree of freedom (χ^2/dof) corresponding to each curve in Figures 2 and 3 are listed in Table 1, which will be discussed later. One can see that the results calculated by the modified Hagedorn function are fitted well with the experimental data.

In order to see clearly the relationship of free parameters (n , T_0 , β_t) and rapidity(y) for J/ψ mesons produced in pp collisions at 5 TeV, 7 TeV and 13 TeV, we plot the parameter values listed in Table 1 in Figure 4. In this Figure, the solid symbols are parameters and the solid lines are our fitted results by the least square method. One can see that one parameter (n) is increased with the rapidity increase, and the other two parameters (T_0 and β_t) are decreased with the rapidity increase. In addition, we find the trend of β_t has an abnormal phenomenon for J/ψ mesons produced in pp collisions at $\sqrt{s}=7$ TeV.

In this paper, we described the transverse momentum distribution of J/ψ mesons produced in pp collisions at the center-of-mass energy 5 TeV, 7 TeV, and 13 TeV by the modified Hagedorn function. From our calculated curves and the experimental data are present in Figures 1–3 and the degree of freedom (χ^2/dof) listed in Table 1, we found that the modified Hagedorn function is good way to study the transverse momentum distribution of J/ψ mesons produced in pp collisions at LHC energy regions. Based on the work of describing the transverse momentum distribution of J/ψ mesons, we extracted the three free parameters (n , T_0 , β_t). As mentioned in literature [10], for point quark–quark scattering $n \approx 4$, and the n parameter gets bigger when multiple scattering centers are involved [10,18–20]. Our research result show the parameter n is increased with the rapidity increase and not obviously different with the collision energy increased at LHC. This result suggests that with the rapidity increased, the more multiple scattering centers are involved. β_t is the average transverse (radial) flow velocity, and T_0 is an estimate for kinetic freeze-out temperature. The two parameters (T_0 and β_t) are decreased with the rapidity increase. This result means that the collision system may be have faster expansion and higher excitation degree in low rapidity region.

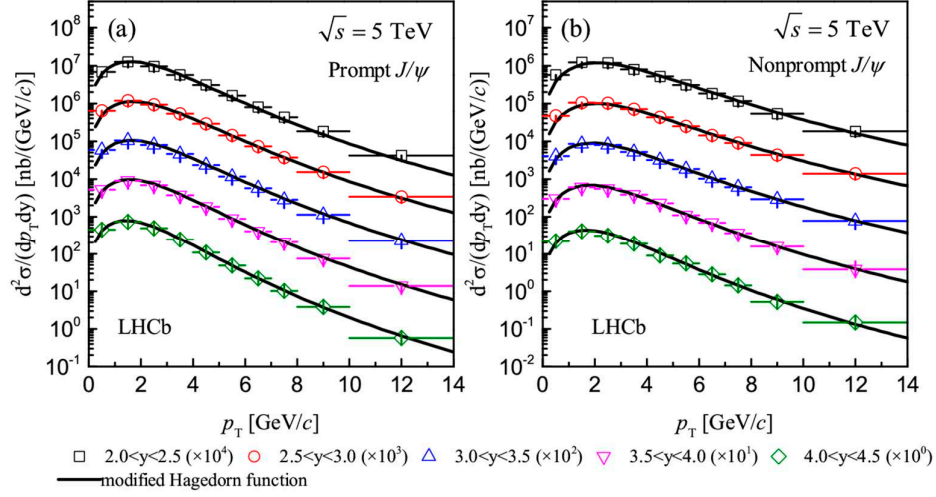


Figure 1. Transverse momentum distribution of (a) prompt J/ψ (b) nonprompt J/ψ mesons produced in pp collisions at $\sqrt{s} = 5$ TeV. The hollow symbols with the error bars represent the experimental data of the LHCb Collaboration in literature [15], the curves are our results calculated by the modified Hagedorn function.

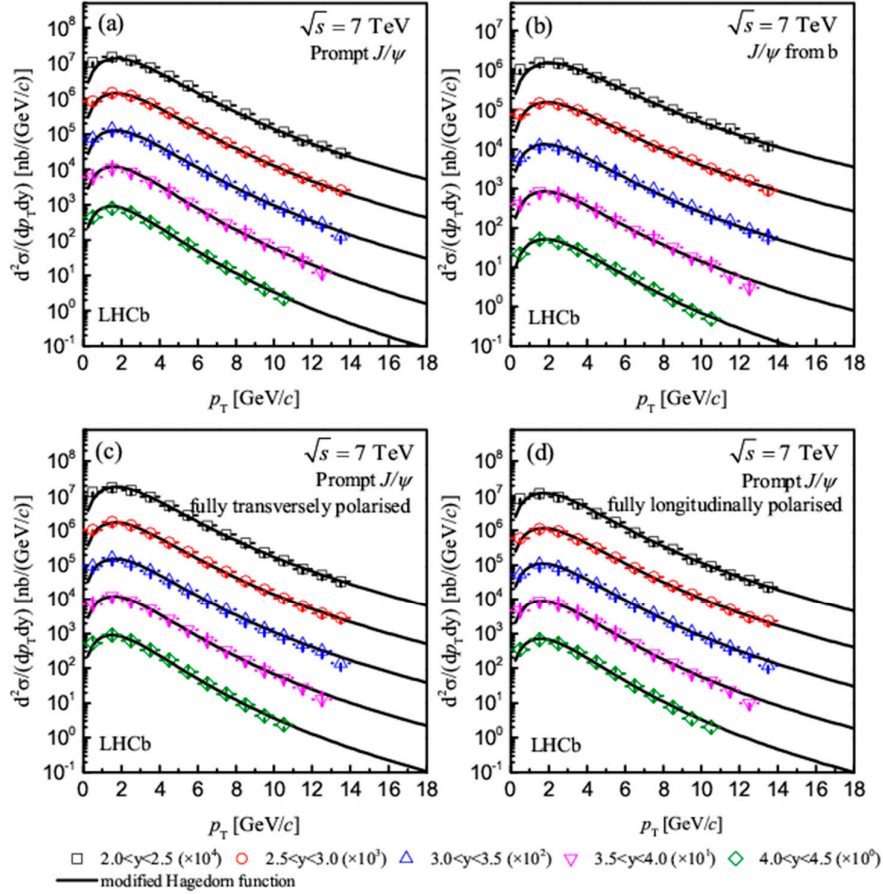


Figure 2. The same as Figure 1, but showing the results of (a) prompt J/ψ (b) J/ψ from b (c) prompt J/ψ (assuming fully transversely polarised) (d) prompt J/ψ (assuming fully longitudinally polarised)

mesons produced in pp collisions at $\sqrt{s} = 7\text{ TeV}$. The experimental data are pouted from the literature [16].

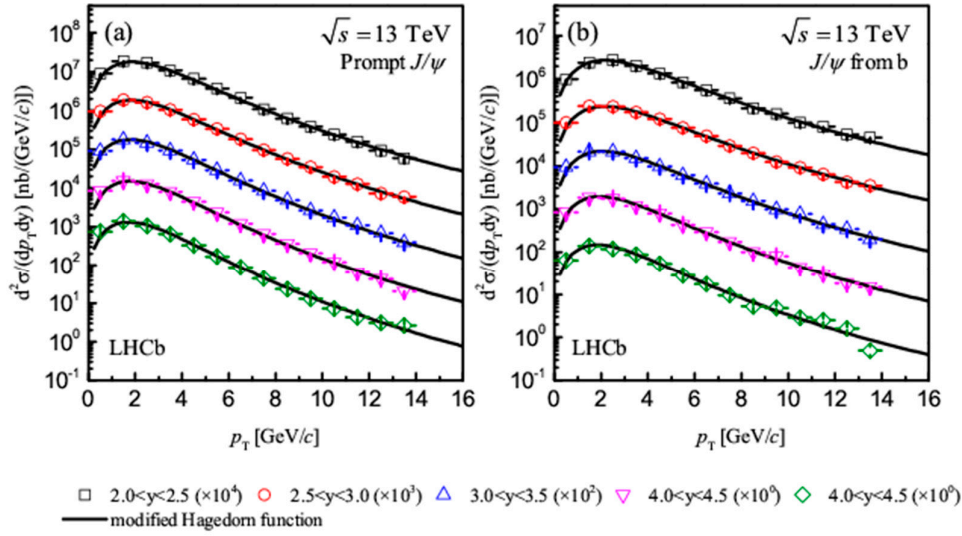


Figure 3. The same as Figure 1, but showing the results of (a) prompt J/ψ (b) J/ψ from b mesons produced in pp collisions at $\sqrt{s} = 13$ TeV. The experimental data are pouted from the literature [17].

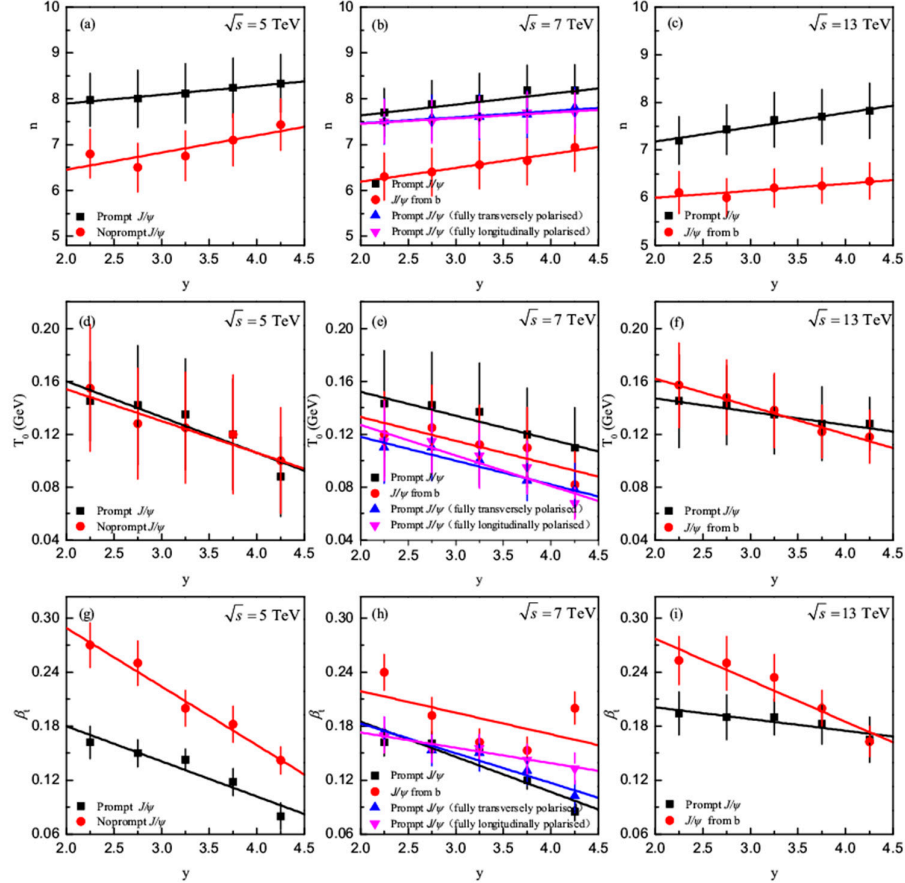


Figure 4. The relationship of free parameters (n , T_0 , β_t) and rapidity(y) for J/ψ mesons produced in pp collisions at 5 TeV, 7 TeV, and 13 TeV. The solid symbols are quoted in Table 2, and the lines are our fitted results by the least square method.

Table 1. Values of parameters and χ^2/dof corresponding to the curves in Figures 1–3.

Figure	Type	n	$T_0(\text{GeV})$	β_t	χ^2/dof	$\langle p_T \rangle (\text{GeV}/c)$	$\sqrt{\langle p_T^2 \rangle}/2 (\text{GeV}/c)$
Figure 1(a)	2.0<y<2.5	975±0.5800	145±0.0300	162±0.018	1.875	2.647±0.051	2.238±0.088
	2.5<y<3.0	000±0.6200	142±0.0450	150±0.015	0.751	2.600±0.042	2.199±0.067
	3.0<y<3.5	120±0.6500	135±0.0420	143±0.012	0.694	2.526±0.023	2.134±0.033
	3.5<y<4.0	243±0.6500	120±0.0420	118±0.015	0.402	2.397±0.014	2.024±0.028
	4.0<y<4.5	335±0.6350	088±0.0300	080±0.015	0.357	2.191±0.032	1.849±0.034
Figure 1(b)	2.0<y<2.5	800±0.5300	155±0.0480	270±0.025	1.467	3.350±0.038	2.840±0.027
	2.5<y<3.0	500±0.5300	128±0.0420	250±0.025	1.672	3.298±0.033	2.809±0.078
	3.0<y<3.5	752±0.5430	125±0.0420	200±0.020	0.379	3.036±0.027	2.592±0.026
	3.5<y<4.0	710±0.5700	120±0.0450	182±0.020	0.333	2.852±0.029	2.428±0.027
	4.0<y<4.5	433±0.5650	100±0.0400	142±0.015	0.883	2.584±0.032	2.196±0.031
Figure 2(a)	2.0<y<2.5	703±0.5220	143±0.0400	162±0.015	1.256	2.706±0.093	2.294±0.104
	2.5<y<3.0	788±0.5200	142±0.0400	161±0.013	0.352	2.657±0.064	2.248±0.100
	3.0<y<3.5	000±0.5500	137±0.0370	152±0.013	0.460	2.590±0.033	2.189±0.053
	3.5<y<4.0	182±0.5500	120±0.0350	120±0.010	0.312	2.414±0.013	2.040±0.012
	4.0<y<4.5	184±0.5560	110±0.0300	085±0.010	0.173	2.300±0.024	1.947±0.013
Figure 2(b)	2.0<y<2.5	303±0.5170	120±0.0320	240±0.020	1.490	3.316±0.075	2.833±0.109
	2.5<y<3.0	400±0.5200	125±0.0320	192±0.020	0.277	3.143±0.062	2.696±0.082
	3.0<y<3.5	555±0.5200	112±0.0300	162±0.015	0.153	2.951±0.037	2.534±0.021
	3.5<y<4.0	648±0.5200	110±0.0300	153±0.015	0.483	2.886±0.035	2.477±0.019
	4.0<y<4.5	935±0.5250	082±0.0250	200±0.018	0.147	2.827±0.021	2.403±0.014
Figure 2(c)	2.0<y<2.5	505±0.5000	110±0.0270	173±0.017	0.823	2.679±0.035	2.270±0.013
	2.5<y<3.0	583±0.5000	110±0.0250	153±0.017	0.440	2.604±0.028	2.208±0.028
	3.0<y<3.5	602±0.5030	100±0.0200	150±0.020	0.690	2.559±0.020	2.169±0.012
	3.5<y<4.0	660±0.5100	085±0.0150	130±0.015	0.578	2.445±0.022	2.072±0.012
	4.0<y<4.5	801±0.4500	078±0.0200	102±0.018	0.227	2.322±0.018	1.967±0.010
Figure 2(d)	2.0<y<2.5	503±0.4770	115±0.0300	170±0.020	0.706	2.688±0.025	2.279±0.036
	2.5<y<3.0	505±0.4700	115±0.0250	155±0.015	0.158	2.646±0.023	2.246±0.029
	3.0<y<3.5	600±0.4500	104±0.0250	156±0.015	0.254	2.588±0.018	2.193±0.011
	3.5<y<4.0	702±0.4500	095±0.0200	143±0.017	0.945	2.500±0.015	2.116±0.013
	4.0<y<4.5	706±0.4740	068±0.0120	133±0.017	0.283	2.386±0.019	2.018±0.014
Figure 3(a)	2.0<y<2.5	202±0.5000	145±0.0350	194±0.024	0.950	2.940±0.037	2.500±0.059
	2.5<y<3.0	430±0.5200	142±0.0300	190±0.025	0.849	2.853±0.022	2.421±0.049
	3.0<y<3.5	632±0.5780	135±0.0300	190±0.020	0.799	2.777±0.012	2.349±0.018
	3.5<y<4.0	701±0.5800	128±0.0280	183±0.023	1.703	2.716±0.005	2.296±0.084
	4.0<y<4.5	820±0.5800	128±0.0200	165±0.025	1.578	2.637±0.003	2.230±0.031
Figure 3(b)	2.0<y<2.5	107±0.4430	157±0.0320	253±0.027	0.439	3.574±0.084	3.055±0.037
	2.5<y<3.0	000±0.4000	148±0.0280	250±0.030	0.540	3.581±0.055	3.065±0.088
	3.0<y<3.5	203±0.4030	138±0.0280	234±0.026	0.608	3.402±0.021	2.912±0.033
	3.5<y<4.0	252±0.3720	122±0.0200	200±0.020	0.529	3.217±0.026	2.762±0.091
	4.0<y<4.5	350±0.3800	118±0.0200	163±0.017	1.909	3.053±0.022	2.629±0.036

Table 2. Values of intercepts, slopes, and χ^2/dof corresponding to the lines in Figures 4 and 5.

Figure	Type	Intercept	Slope	χ^2/dof
Figure 4(a)	prompt J/ψ	7.509±0.057	0.193±0.017	0.003
	noprompt J/ψ	5.703±0.429	0.374±0.129	0.193
Figure 4(b)	prompt J/ψ	7.168±0.101	0.253±0.030	0.010
	J/ψ from b	5.585±0.111	0.302±0.033	0.014
	prompt J/ψ (fully transversely polarized)	7.195±0.067	0.134±0.020	0.006
	prompt J/ψ (fully longitudinally polarized)	7.211±0.064	0.121±0.019	0.006
Figure 4(c)	prompt J/ψ	6.577±0.108	0.301±0.033	0.012
	J/ψ from b	5.703±0.141	0.148±0.042	0.035
Figure 4(d)	prompt J/ψ	0.214±0.019	-0.027±0.006	0.095
	noprompt J/ψ	0.202±0.014	-0.024±0.004	0.029
Figure 4(e)	prompt J/ψ	0.188±0.010	-0.018±0.003	0.021
	J/ψ from b	0.169±0.018	-0.018±0.005	0.116
	prompt J/ψ (fully transversely polarized)	0.154±0.008	-0.018±0.002	0.041
	prompt J/ψ (fully longitudinally polarized)	0.173±0.015	-0.023±0.005	0.252
Figure 4(f)	prompt J/ψ	0.167±0.004	-0.010±0.001	0.008
	J/ψ from b	0.204±0.005	-0.021±0.002	0.020
Figure 4(g)	prompt J/ψ	0.258±0.021	-0.039±0.006	0.684
	noprompt J/ψ	0.419±0.015	-0.065±0.005	0.145
Figure 4(h)	prompt J/ψ	0.263±0.026	-0.039±0.008	1.336
	J/ψ from b	0.267±0.061	-0.024±0.018	3.890
	prompt J/ψ (fully transversely polarized)	0.249±0.014	-0.033±0.004	0.172
	prompt J/ψ (fully longitudinally polarized)	0.207±0.007	-0.017±0.002	0.072
Figure 4(i)	prompt J/ψ	0.227±0.011	-0.013±0.003	0.071
	J/ψ from b	0.369±0.025	-0.046±0.007	0.339
Figure 5(a)	prompt J/ψ	3.197±0.106	-0.223±0.032	5.515
	noprompt J/ψ	4.310±0.122	-0.396±0.037	3.867
Figure 5(b)	prompt J/ψ	3.219±0.079	-0.211±0.024	1.735
	J/ψ from b	3.827±0.106	-0.247±0.032	3.345
	prompt J/ψ (fully transversely polarized)	3.089±0.052	-0.157±0.016	1.976
	prompt J/ψ (fully longitudinally polarized)	3.049±0.049	-0.150±0.015	1.941
Figure 5(c)	prompt J/ψ	3.268±0.014	-0.149±0.004	0.639
	J/ψ from b	4.279±0.121	-0.281±0.036	2.582
Figure 5(d)	prompt J/ψ	2.708±0.090	-0.191±0.027	1.809
	noprompt J/ψ	3.658±0.115	-0.334±0.035	3.347
Figure 5(e)	prompt J/ψ	2.730±0.063	-0.180±0.019	1.212
	J/ψ from b	3.290±0.072	-0.216±0.022	3.840
	prompt J/ψ (fully transversely polarized)	2.619±0.045	-0.148±0.013	4.597
	prompt J/ψ (fully longitudinally polarized)	2.594±0.043	-0.130±0.013	2.625
Figure 5(f)	prompt J/ψ	2.791±0.015	-0.133±0.005	0.121
	J/ψ from b	3.635±0.101	-0.231±0.030	1.463

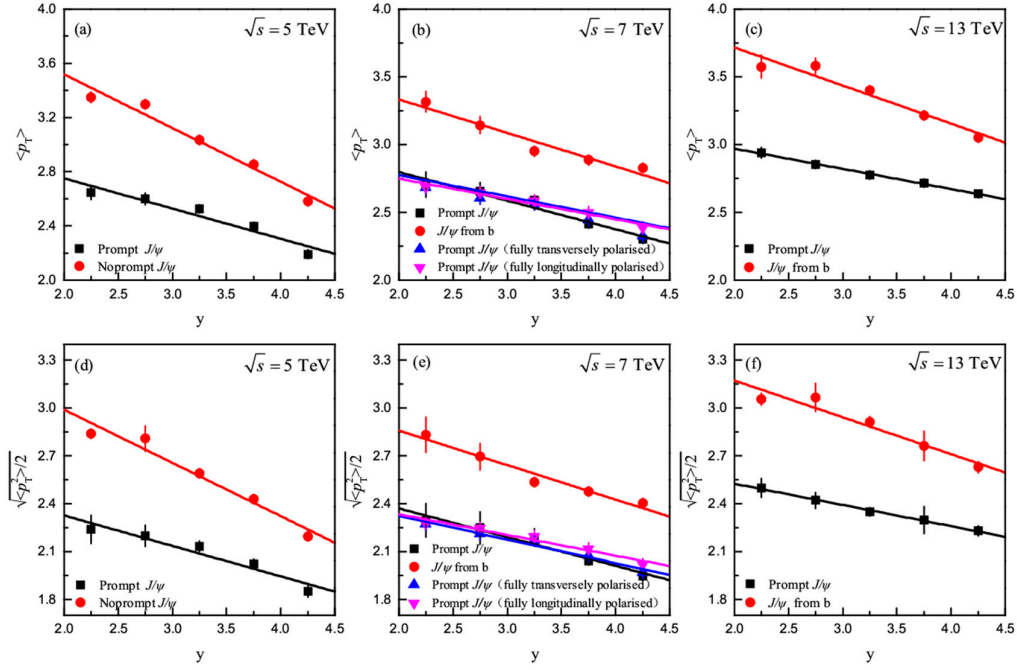


Figure 5. The same as Figure 4, but showing the relationship between physical quantity ((a)-(c) $\langle p_T \rangle$

, (d)-(f) $\sqrt{\langle p_T^2 \rangle}$) and y for J/ψ mesons produced in pp collisions at 5 TeV, 7 TeV, and 13 TeV.

Data Availability Statement: All data are quoted from the mentioned references. As a phenomenological work, this paper does not report new data.

Acknowledgments: Author Li-Na Gao acknowledges the financial support from the National Natural Science Foundation of China under Grant No. 11847003, the Shanxi Provincial Science and Technology Innovation Plan under Grant No. 2019L0804, the university student innovation and entrepreneurship training program of Taiyuan Normal University No. CXCX 2276, the Doctoral Scientific Research Foundation of Taiyuan Normal University under Grant No. I170167, and the Doctoral Scientific Research Foundation of Shanxi Province under Grant No. I170269.

Conflicts of Interest: The authors declare that there are no conflicts of interest regarding the publication of this paper.

Reference

1. P. Moreau, O. Soloveva, and I. Grishmanovskii et al.. Properties of the QGP created in heavy-ion collisions [J]. *Astronomische Nachrichten*, 2021, 342, 715-726.
2. C. A. Graeff, M. D. Alloy, and K. D. Marquez et al.. Hadron-quark phase transition: the QCD phase diagram and stellar conversion [J]. *Journal of Cosmology and Astroparticle Physics*, 2019, 2019, 024
3. S. Domdey, B. Z. Kopeliovich, and H. J. Pirner. Jet-evolution in the quark-gluon plasma from RHIC to the LHC [J]. *Nuclear Physics A*, 2011, 856, 134-153.
4. L. N. Gao, Fu-Hu Liu and Roy A. Lacey. Excitation functions of parameters in Erlang distribution, Schwinger mechanism, and Tsallis statistics in RHIC BES program. *The European Physical Journal A*, 2016, 52, 137.
5. L. N. Gao and Fu-Hu Liu. Comparing Erlang Distribution and Schwinger Mechanism on Transverse Momentum Spectra in High Energy Collisions. *Advances in High Energy Physics*, 2016, 2016, 1505823.
6. L. N. Gao, Fu-Hu Liu, and Bao-Chun Li. Rapidity Dependent Transverse Momentum Spectra of Heavy Quarkonia Produced in Small Collision Systems at the LHC. *Advances in High Energy Physics*. 2019, 2019, 6739315.
7. L. N. Gao, Fu-Hu Liu. Transverse momentum spectra of heavy baryons and mesons in forward rapidity range in small collision system at the LHC. *Indian Journal of Physics*. 2020, 94, 1431-1450.

8. L. N. Gao, Er-Qin Wang. Transverse momenta and pseudo-rapidity spectrum of the top quark, lepton and b jet in proton-proton collisions at LHC. *Advances in High Energy Physics*, 2021, 2021, 6660669.
9. R. Hagedorn. Multiplicities, pr distributions and the expected hadron→ quark-gluon phase transition [J]. *Rivista del Nuovo Cimento*, 1983, 6(CERN-TH-3684), 1.
10. K. K. Olimov, F. H. Liu, and K.A. Musaev et al.. Multiplicity dependencies of midrapidity transverse momentum spectra of identified charged particles in $p+p$ collisions at $(s)^{1/2}=13$ TeV at LHC. *International Journal of Modern Physics A*, 2021, 36, 2150149.
11. P. K. Khandai, P. Sett, and P. Shukla et al.. System size dependence of hadron pT spectra in $p+p$ and Au+Au collisions at $\sqrt{s_{NN}} = 200$ GeV [J]. *Journal of Physics G*, 2014, 41, 025105.
12. K. K. Olimov, A. Iqbal, and S. Masood. Systematic analysis of midrapidity transverse momentum spectra of identified charged particles in $p+p$ collisions at $\sqrt{s_{NN}} = 2.76, 5.02$, and 7 TeV at the LHC [J]. *International Journal of Modern Physics A*, 2020, 35, 2050167.
13. K. K. Olimov, S. Z. Kanokova, and A. K. Olimov et al.. Combined analysis of midrapidity transverse momentum spectra of the charged pions and kaons, protons and antiprotons in $p+p$ and Pb+ Pb collisions at $\sqrt{s_{NN}} = 2.76$ and 5.02 TeV at the LHC [J]. *Modern Physics Letters A*, 2020, 35, 2050237.
14. K. K. Olimov, S. Z. Kanokova, and K. Olimov et al.. Average transverse expansion velocities and global freeze-out temperatures in central Cu+Cu, Au+Au, and Pb+Pb collisions at high energies at RHIC and LHC [J]. *Modern Physics Letters A*, 2020, 35, 2050115.
15. R. Aaij, A.S.W. Abdelmotteleb, and C. Abellán Beteta et al.. Measurement of J/ψ production cross-sections in pp collisions at $\sqrt{s} = 5$ TeV [J]. *Journal of High Energy Physics*, 2021, 11, 181.
16. R. Aaij, B. Adeva, and M. Adinolfi et al.. Measurement of J/ψ production in pp collisions at $\sqrt{s} = 7$ TeV [J]. *The European Physical Journal C*, 2011, 71, 1645.
17. R. Aaij, B. Adeva, and M. Adinolfi et al.. Measurement of forward J/ψ production cross-sections in pp collisions at $\sqrt{s} = 13$ TeV [J]. *Journal of High Energy Physics*, 2015, 10, 172.
18. P. K. Khandai, P. Sett, and P. Shukla et al.. Hadron spectra in $p+p$ collisions at RHIC and LHC energies [J]. *International Journal of Modern Physics A*, 2013, 28, 1350066.
19. R. Blankenbecler, S. J. Brodsky, and J. Gunion. Analysis of particle production at large transverse momentum [J]. *Physical Review D*, 1975, 12, 3469.
20. S. J. Brodsky, H. J. Pirner, and J. Raufeisen. Scaling properties of high pr inclusive hadron production [J]. *Physics Letters B*, 2006, 637, 58.

Disclaimer/Publisher's Note: The statements, opinions and data contained in all publications are solely those of the individual author(s) and contributor(s) and not of MDPI and/or the editor(s). MDPI and/or the editor(s) disclaim responsibility for any injury to people or property resulting from any ideas, methods, instructions or products referred to in the content.